Applied Physics Letters

Undulate microarray fabrication on polymer film using standing surface acoustic waves and ultraviolet polymerization

Cite as: Appl. Phys. Lett. **108**, 241911 (2016); https://doi.org/10.1063/1.4954233
Submitted: 05 April 2016 . Accepted: 07 June 2016 . Published Online: 15 June 2016

Deqing Mei, Dai Xue, Yancheng Wang, and Shaochen Chen

Undulate microarray fabrication on polymer film using standing surface acoustic waves and ultraviolet polymerization

Deqing Mei,[1,2,a)] Dai Xue,[1,2] Yancheng Wang,[1,2] and Shaochen Chen[3]
[1]*State Key Laboratory of Fluid Power and Mechatronic Systems, College of Mechanical Engineering, Zhejiang University, Hangzhou 310027, China*
[2]*Key Laboratory of Advanced Manufacturing Technology of Zhejiang Province, College of Mechanical Engineering, Zhejiang University, Hangzhou 310027, China*
[3]*Department of NanoEngineering, University of California, San Diego, California 92093, USA*

(Received 5 April 2016; accepted 7 June 2016; published online 15 June 2016)

By exciting standing surface acoustic waves (SAWs), a monomer solution can be shaped into a wavy structure. By applying ultraviolet (UV) polymerization, a linear undulate microarray can be fabricated on the polymer material using one-dimensional standing SAWs. When two-dimensional standing SAWs are applied, a latticed microarray, which presents periodically distributed bumps and wells, can be fabricated. The periodicity of the undulate microarray is dependent on the SAW wavelength. Also, the undulating amplitude of the microarray is tunable when applying different input voltages to generate SAWs. The integrated standing SAWs and UV polymerization process provide a rapid method for creating periodic surface patterns. *Published by AIP Publishing.*
[http://dx.doi.org/10.1063/1.4954233]

Due to the high biocompatibility and the ability to be easily composited with functional materials, biopolymers equipped with surface microarrays have current and potential applications in biomedical and microelectronic fields. Taking tissue engineering as examples, the use of hydrogel polymers to fabricate cell-laden substrates with specialized surface microarray provides a workable way to evaluate the effects of morphology on cell encapsulation *in vitro*.[1–3] To mimic the vascular morphology, hydrogel-based microchips with artificially branched channels are designed and fabricated to study the physical behaviours of cells.[4–7] Polymer substrates with surface bumps or wells have the ability to pattern proteins,[8] cells and DNAs,[9,10] or to form reaction vessels and detector elements for biosensors.[11] In addition to biomedical applications, polymer-based microarrays also offer unique properties needed for fabricating composite piezoelectric materials and dielectric layers.[12,13] Photolithography is the primary technique for fabricating planar microarrays. Dynamic projection printing is an emerging technique that has demonstrated its ability to fabricate complex user-defined microstructures with diverse materials. However, these techniques need physical or chemical templating, and therefore, result in long fabrication times. In addition, current techniques fail to obtain microarrays with continuous and smooth surfaces; this is attributed to principle errors such as the step effect.

On the other hand, the ability to generate surface patterns through surface acoustic waves (SAWs) has been recently demonstrated. Qi and Tan presented numerical studies of the capillary waves generated by traveling SAWs, and found that the interval between two antinodes on the fluid surface is about the half SAW wavelength.[14,15] SAW can be generated by applying a sinusoidal voltage on an interdigital transducer (IDT) that deposits on a lithium niobate ($LiNO_3$) single-crystal piezoelectric substrate.[16] Recently, SAWs have been applied in microfluidic systems, including drop control,[17,18] micro-atomizers,[19] particle manipulation,[20–22] and other actuators.[23,24] These SAW devices have advantages including low cost, being easily miniaturized, highly biocompatible, and energy efficient.[25] We note that SAW related studies have mainly been focused on fluid and particle manipulation, and not for using SAW to fabricate microstructures.

Here, we present a method for fabricating undulate microarrays using combination of standing SAWs and ultraviolet (UV) polymerization. The undulate microarrays result from solidifying standing SAWs excited ordered surface patterns on photosensitive polymer films. As the patterns are independently controlled by standing SAWs-induced acoustic pressure, we can fabricate diverse undulate microarrays using different kinds of standing SAWs. First, one-dimensional (1D) standing SAWs under different wavelengths are used to fabricate linear undulate microarrays. The linear microarray has an approximately sine-shaped surface, and the period is roughly equal to the half SAW wavelength. Moreover, we are able to change the undulation amplitude of microarrays by applying different input voltages to generate standing SAWs. Then, two-dimensional (2D) standing SAWs are used to fabricate latticed undulate microarrays. These possess a series of periodically distributed bumps and wells, and the interval of each bump or well is also close to the half SAW wavelength. Compared with conventional techniques, this standing SAWs-based method does not require templating and can produce smooth surface contours.

SAW propagates along the piezoelectric substrate surface, and their energy is confined to the depth of a few wavelengths beneath the surface. Overlap of two series of identical SAWs or four series of orthogonal SAWs can form the 1D or 2D standing SAW, respectively, as well as uniformly distributed vibration areas on the substrate. The areas with minimum vibration amplitude are wave nodes, and the areas with maximum vibration amplitude are known as wave antinodes.

[a)]Author to whom correspondence should be addressed. Electronic mail: meidq_127@zju.edu.cn.

The locations of wave nodes and antinodes are fixed once the SAWs are generated. Fig. 1(a) shows the 1D standing SAW on $LiNO_3$ substrate. Although the SAW amplitude is 1–10 nm, the surface acceleration is so huge that it can excite strong longitudinal waves in the fluid on top of the substrate, and generate an acoustic pressure field. Air-fluid free surface is destabilized by the acoustic pressure; as a consequence, ordered patterns are emerged on the surface under the interference of continuous acoustic pressure from the standing SAW. According to the relationship between acoustic pressure field in the fluid and the location of wave nodes and antinodes on the substrate, we assume that the ordered pattern has the same regularity as the standing SAW, as demonstrated in Fig. 1(b). In doing so, we can obtain different ordered patterns on the air-fluid free surface by changing the working parameters of the standing SAWs.

Fig. 2(a) illustrates the experimental configuration of a 1D standing SAW-based fabrication device that has one pair of parallel IDTs. A hydrophilic photo-sensitive polymer is coated evenly on the $LiNO_3$ substrate. There is a PDMS (Polydimethylsiloxane) chamber with nitrogen inlet and outlet covering the entire polymer film, which provides an oxygen-free atmosphere to eliminate the inhibition of UV polymerization during solidification. Absorption bands are placed at each end of the IDT with the purpose of preventing wave reflection from the substrate edges. Once the ordered pattern has emerged on the film surface, we can use UV light to solidify the polymer film and then obtain the microarray. Our standing SAW-based fabrication technique can be extended to fabricate latticed undulate microarrays. Fig. 2(b) shows a schematic of the 2D standing SAW-based fabrication device containing two pairs of orthogonal IDTs. As the time taken to generate the pattern is negligible, and the duration of polymerization is considerably short, the whole fabrication process can be accomplished within several seconds.

IDTs with straight electrodes are fabricated onto a double-polished 128° Y-cut, X-propagating $LiNO_3$ (500 μm thick) substrate through standard lithography and lift-off techniques. The IDTs in both devices have 30 straight finger pairs with space ratio of 1:1, and the wavelength of the excited SAW equals four times the width of electrode (or

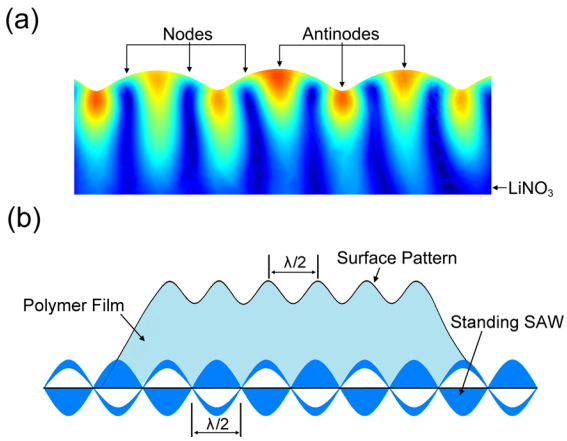

FIG. 1. (a) 1D standing SAW generated on the $LiNO_3$ substrate. (b) Interaction of a standing SAW with polymer film excites ordered surface pattern on the air-fluid free surface; λ denotes SAW wavelength (drawings are not in scale).

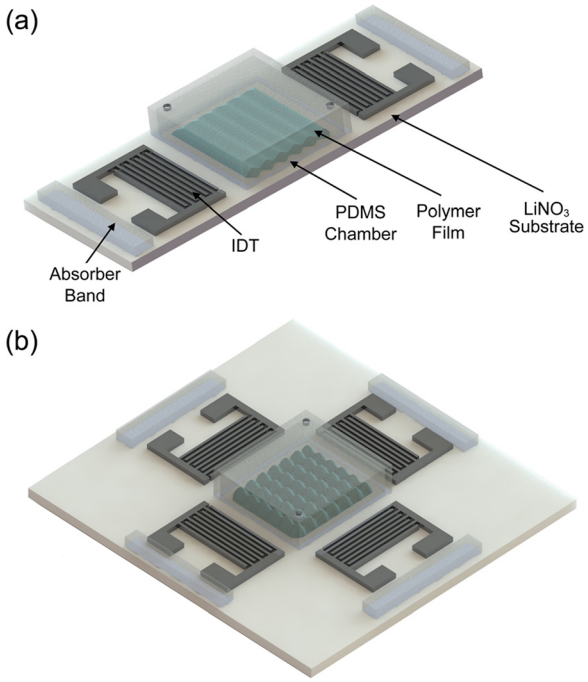

FIG. 2. Schematic diagram of the (a) 1D SAW-based device for fabricating linear undulate microarrays and (b) 2D standing SAW-based device for fabricating latticed undulate microarrays. Ordered surface patterns are excited in both devices (drawings are not in scale).

gap). Hydrophilic poly (ethylene glycol) diacrylate (PEGDA, 700 Da, Sigma, USA) is used as the pre-polymer because of the good wettability with $LiNO_3$ substrate. Irgacure 2959 (Sigma, USA), serving as the photoinitiator, is mixed with pre-polymer at PEGDA [99% (w/v)]+Irgacure 2959 [1% (w/v)] to acquire the photo-sensitive polymer. The polymer is sonicated for 3 h prior to coating and UV polymerization.[26] Continuous sinusoidal voltages, generated by an waveform generator (33522B, Agilent, USA), are applied on IDTs through customized SMA pedestals to excite SAWs directly. The PEGDA monomer solution is transferred onto the substrate through a micropipette and finally solidified by 365 nm UV light from an LED (Light Emitting Diode) array. We employ a laser scanning confocal microscope (OLS4100, Olympus, Japan) to acquire images and data from the two types of undulate microarray.

According to Guo's study,[27] when two or four series of traveling SAWs are superposed on the substrate, the time-averaged 1D and 2D acoustic pressure distributions in the x and y directions can be given as

$$P_{1D}^2 = P_x^2 \sin^2[k_x(x_0 - x)], \quad (1)$$

$$P_{2D}^2 = P_x^2 \sin^2[k_x(x_0 - x)] + P_y^2 \sin^2[k_y(y_0 - y)], \quad (2)$$

where k_x and k_y, P_x and P_y are the wave numbers and acoustic amplitudes in directions x and y, respectively. The x_0 and y_0 mean the distance between two pairs of opposite IDTs. By substituting the k_x, k_y, x_0, and y_0 into Eqs. (1) and (2), and let the P_x and P_y equal 1, we can calculate the acoustic pressure distributions in x-y plane. Fig. 3(a) shows the time-averaged calculated acoustic pressure distribution of the 1D standing SAW under the wavelength of 140 μm, where we can see that the nodes (black) or antinodes (white) are aligned as multiple

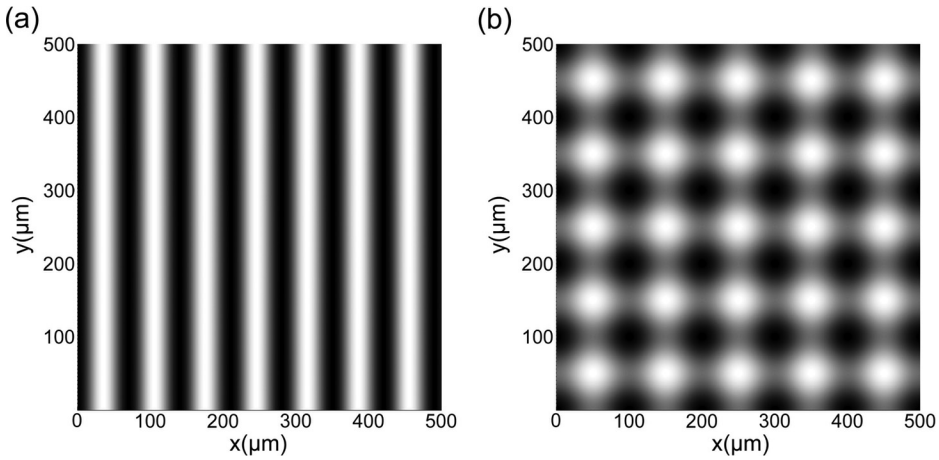

FIG. 3. (a) Calculated time-averaged acoustic pressure distribution of the 1D standing SAW under the wavelength of 140 μm and (b) 2D standing SAW under the wavelength of 200 μm. The scale runs from black at minimum to white at maximum.

stripes. These stripes are parallel to the SAW front, and the interval of adjacent nodes or antinodes is about equal to the half SAW wavelength, which is 70 μm. The calculated acoustic pressure distribution of 2D standing SAW, with the wavelength of 200 μm, is shown in Fig. 3(b). The nodes and antinodes are formed into a dot matrix with an interval of 100 μm.

We first adopt the 1D standing SAW under a wavelength of 140 μm and input voltage of 7 V_{pp} to fabricate the linear undulate microarrays. A laser snapshot of the linear microarray is shown in Fig. 4(a), and the stripes refer to the crests and troughs in the microarray. The measured interval of adjacent crests or troughs is about 70 μm, which shows perfect consistency with the period of calculated acoustic distribution. From Fig. 4(b), we can see that the linear undulate microarray has an approximately sine-shaped surface, and the measured average undulation amplitude is 3.2 μm. During the experiments, we noticed that the surface patterns are definitely affected by film thickness. If the film is too thick, the acoustic pressure is too weak to destabilize the surface, and

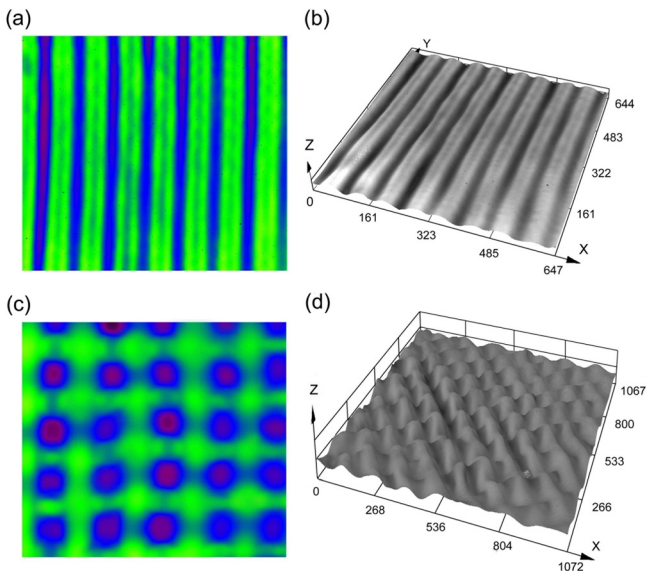

FIG. 4. (a) Laser snapshot displays seven crests and troughs in linear microarray. (b) Scanning image shows the linear microarray with an approximately sine-shaped surface. (c) Laser snapshot shows the amplitude distribution of latticed microarrays. (d) Scanning image displays periodically distributed bumps and wells. The scale is magnified three times in the *Z*-direction.

weak streaming is excited in the film. In contrast, when the film is too thin, the acoustic pressure would lead to film rupture. The film thickness in each experiment is about 40 μm. Furthermore, we achieve changes in undulation amplitude from about 3 μm to over 5 μm by increasing the input voltage. In addition, we use 1D standing SAWs under wavelengths of 156 and 200 μm to fabricate the linear undulate microarrays. The periods of each linear microarray are approximately equal to 78 and 100 μm, respectively, which show a good consistence with the calculated results under the wavelength of 156 and 200 μm. These linear microarrays resulting from different devices indicate that the undulation periodicity depend on the SAW wavelength and reveal the possibility for the fabrication of microarrays with different sizes.

With the accomplishment in using 1D standing SAWs to fabricate linear microarrays where the surface patterns extend along a single direction, we hypothesize that 2D standing SAWs may be able to destabilize polymer film in two orthogonal directions and give rise to latticed microarrays. Then, 2D standing SAWs under the wavelength of 200 μm is applied to fabricate undulate microarray. The undulation amplitude of the latticed microarray presents a quadrilateral closed-packed distribution, as demonstrated in Fig. 4(c). The measured period is about 100 μm, which matches the half SAW wavelength. From Fig. 4(d), we can clearly observe periodically distributed bumps, and the average undulation amplitude is 15.6 μm. It is worth noting that there are also distributed wells, which are alternately distributed and located among four bumps.

Comparing the acoustic distributions with the microarrays, we find that the linear and latticed feature is decided by the dimensions of standing SAWs, and the period of microarray can be adjusted by the SAW wavelength. Further, the period of microarray is about equal to the half SAW wavelength. Hence, we can use the calculated acoustic pressure distributions to predict the regularity and periodicity of the microarrays. The acoustic pressure distribution in the polymer film is generated by the standing SAWs on the $LiNO_3$ substrate. Due to the absence of complex wave reflection and attenuation, the interference to acoustic distribution in the polymer film is negligible. Therefore, the periodicity of acoustic distribution in the *x*-*y* plane can be adjusted by SAW wavelength. In the acoustic field that contains periodical nodes and antinodes, the positions and directions of the induced acoustic pressure are settled and also periodically

distributed. It is the distributed acoustic pressures that disturb the polymer film and subsequently excite the patterns. Above all, we can change the period of microarrays by using standing SAW with different wavelengths, and the period is about equal to the half SAW wavelength. Except for the standing SAWs parameters, the properties of polymer, such as density and surface tension, have some effects on the amplitude and profile of the crests, troughs in linear microarrays and bumps, and wells in latticed microarrays. We think that the fully and accurate conditions should be introduced to predict the microarrays, and this will be our future work.

We have demonstrated a rapid method for undulate microarray fabrication by integrating standing SAWs with UV polymerization. Linear undulate microarrays with periods of time about 70, 78, and 100 μm and latticed undulate microarrays with period that close to 100 μm have been fabricated. The results highlight the possibility for rapid and controllable fabrication of surface patterns without requiring the use of templating and expensive instruments. By adjusting the frequency and input voltage, the periodicity and amplitude of undulate microarrays can be controlled. These polymer based microarrays can be used for making a variety of devices in biomedicine, optics, and electronics.

This work was financially supported by the National Basic Research Program (973) of China (Grant No. 2011CB013300), the National Natural Science Foundation of China (Grant No. 51575482), the Science Fund for Creative Research Groups of National Natural Science Foundation of China (Grant No. 51521064), and the Program for New Century Excellent Talents in University (Grant No. NCET-13-0518).

[1]P. Soman, P. H. Chung, A. P. Zhang, and S. Chen, Biotechnol. Bioeng. **110**(11), 3038 (2013).
[2]J. W. Nichol, S. T. Koshy, H. Bae, C. M. Hwang, S. Yamanlar, and A. Khademhosseini, Biomaterials **31**(21), 5536 (2010).
[3]A. Agarwal, Y. Farouz, A. P. Nesmith, L. F. Deravi, M. L. McCain, and K. K. Parker, Adv. Funct. Mater. **23**(30), 3738 (2013).
[4]T. Q. Huang, X. Qu, J. Liu, and S. Chen, Biomed. Microdevices **16**(1), 127 (2014).
[5]J. Wu, C.-H. Yu, S. Li, B. Zou, Y. Liu, X. Zhu, Y. Guo, H. Xu, W. Zhang, and L. Zhang, Langmuir **31**(3), 1210 (2015).
[6]P. Costa, J. E. Gautrot, and J. T. Connelly, Acta Biomater. **10**(6), 2415 (2014).
[7]W. Zheng and X. Jiang, Colloids Surf., B **124**, 97 (2014).
[8]R. S. Kane, S. Takayama, E. Ostuni, D. E. Ingber, and G. M. Whitesides, Biomaterials **20**(23), 2363 (1999).
[9]S. Iwanaga, Y. Akiyama, A. Kikuchi, M. Yamato, K. Sakai, and T. Okano, Biomaterials **26**(26), 5395 (2005).
[10]S. A. Lange, V. Benes, D. P. Kern, J. K. H. Hörber, and A. Bernard, Anal. Chem. **76**(6), 1641 (2004).
[11]G. Steiner, C. Zimmerer, and R. Salzer, Langmuir **22**(9), 4125 (2006).
[12]G. Liang, Y. Wang, D. Mei, K. Xi, and Z. Chen, JMemS **24**(5), 1510 (2015).
[13]K. Kim, W. Zhu, X. Qu, C. Aaronson, W. R. McCall, S. Chen, and D. J. Sirbuly, ACS Nano **8**(10), 9799 (2014).
[14]A. Qi, L. Y. Yeo, and J. R. Friend, Phys. Fluids **20**(7), 074103 (2008).
[15]M. K. Tan, J. R. Friend, O. K. Matar, and L. Y. Yeo, Phys. Fluids **22**(11), 112112 (2010).
[16]R. M. White and F. W. Voltmer, Appl. Phys. Lett. **7**(12), 314 (1965).
[17]A. Wixforth, C. Strobl, Ch. Gauer, A. Toegl, J. Scriba, and Z. V. Guttenberg, Anal. Bioanal. Chem. **379**(7–8), 982 (2004).
[18]A. Renaudin, P. Tabourier, J.-C. Camart, and C. Druon, J. Appl. Phys. **100**(11), 116101 (2006).
[19]K. Chono, N. Shimizu, Y. Matsui, J. Kondoh, and S. Shiokawa, Jpn. J. Appl. Phys., Part 1 **43**(5B), 2987 (2004).
[20]X. Ding, Sz.-C. S. Lin, B. Kiraly, H. Yue, S. Li, I.-K. Chiang, J. Shi, S. J. Benkovic, and T. J. Huang, Proc. Natl. Acad. Sci. **109**(28), 11105 (2012).
[21]J. Zhang, L. Meng, F. Cai, H. Zheng, and C. R. P. Courtney, Appl. Phys. Lett. **104**(22), 224103 (2014).
[22]C. D. Wood, J. E. Cunningham, R. O'Rorke, C. Wälti, E. H. Linfield, A. G. Davies, and S. D. Evans, Appl. Phys. Lett. **94**(5), 054101 (2009).
[23]R. J. Shilton, N. R. Glass, P. Chan, L. Y. Yeo, and J. R. Friend, Appl. Phys. Lett. **98**(25), 254103 (2011).
[24]R. J. Shilton, S. M. Langelier, J. R. Friend, and L. Y. Yeo, Appl. Phys. Lett. **100**(3), 033503 (2012).
[25]X. Ding, P. Li, Sz.-C. S. Lin, Z. S. Stratton, N. Nama, F. Guo, D. Slotcavage, X. Mao, J. Shi, and F. Costanzo, Lab Chip **13**(18), 3626 (2013).
[26]K. C. Hribar, P. Soman, J. Warner, P. Chung, and S. Chen, Lab Chip **14**(2), 268 (2014).
[27]F. Guo, P. Li, J. B. French, Z. Mao, H. Zhao, S. Li, N. Nama, J. R. Fick, S. J. Benkovic, and T. J. Huang, Proc. Natl. Acad. Sci. U. S. A. **112**(1), 43 (2015).